PROCEEDINGS, Thirty-Eighth Workshop on Geothermal Reservoir Engineering
Stanford University, Stanford, California, February 11-13, 2013
SGP-TR-198

DEVELOPMENT OF EXPLORATION METHODS FOR ENGINEERED GEOTHERMAL SYSTEMS THROUGH INTEGRATED GEOPHYSICAL, GEOLOGIC AND GEOCHEMICAL INTERPRETATION

THE SEISMIC ANALYSIS COMPONENT

Ileana M. Tibuleac[1], Joe Iovenitti[2], David von Seggern[1], Jon Sainsbury[2], Glenn Biasi[1] and John G. Anderson[1]

[1]University of Nevada, Reno, Nevada Seismological Laboratory,
1664 N'th Virginia St., MS 174,
Reno, NV, USA 89557
e-mail: imtseismic@yahoo.com
[2]AltaRock Energy Inc.
2320 Marinship Way, 2nd Floor
Sausalito, CA, USA 94965
e-mail: jiovenitti@altarockenergy.com

ABSTRACT

The primary objective of this study is to develop and test the seismic component of a calibrated exploration method that integrates geological, geophysical, and geochemical data to identify potential drilling targets for Engineered Geothermal Systems (EGS). In exploring for EGS sites, the primary selection criteria identified by the AltaRock Energy, Inc. (AltaRock) Team are, in order of importance, (1) temperature, (2) rock type at the depth of interest; and (3) stress regime. The core exploration methodology we develop for this project is a new seismic technique which uses complementary information derived from regional tomographic models of body (*P* and *S*) and surface waves, statistically integrated with seismic velocity models derived from ambient noise to predict temperature and rock type. Using the new estimated seismic velocity models, we test the supposition that the uncertainty and the degree of non-uniqueness in predictions of temperature and rock type from the seismic data could be reduced by integration with other geophysical and geochemical data into an EGS conceptual model that will form the basis of an exploration methodology. The new method is applied to the EGS Exploration Methodology Project Area in Dixie Valley, NV, (DVSA) one of the best characterized geothermal areas in the Basin and Range, also known for relatively low seismic activity between large seismic events.

INTRODUCTION

The objective of the seismic investigation is to estimate a high resolution (~ 5 km^2) *P/S* seismic velocity model in the Dixie Valley Study Area (DVSA), the EGS Exploration Methodology Project Area, using new, and baseline information, from independent sources. Our studies focus on extracting maximum information in the Dixie Valley Geothermal Well field area, also referred to as the calibration area (Figure 1). In order to develop the required data for the DVSA, a larger region referred to as the Dixie Valley Extended Study Area (DVESA) needs to be assessed (Figure 2).

The initial publicly available information review concluded that improved *P/S* seismic velocity model resolution in DVSA was required. A dense seismic array (21 three-component, broadband sensors, with an overall array aperture of 45 km) was installed in two deployments, each having a three-month duration. Ambient seismic noise and signal rather than active sources are used to retrieve inter-station and same-station Green's Functions (GFs), to be used for subsurface imaging. Another innovative aspect of the seismic work is to determine if estimating the GF *P*-reflection component beneath the stations from noise auto-correlation could be used to image the substructure. We report results of applying the technique to estimate a *P/S* velocity model from the GF surface wave components and from the GF body-wave reflection component, retrieved from ambient noise and signal cross-correlation and auto-correlation beams. Using seismic velocity models to infer temperature will be statistically assessed, in combination with other geophysical technique results.

METHOD

Figure 3 shows an outline of the major tasks in our study and of the analysis method, which was first tested in the Reno, NV area (Tibuleac, in prep. for *Seismological Research Letters*). To prepare for the inversion of the final DVSA model we created an input model (DVSA_INITIAL_MOD) as a superposition of independently-estimated models described

below: (1) the baseline *P/S* velocity seismic model (DVESA_BL_MOD), (2) the low resolution *P/S*-velocity ambient - noise estimated model (DVESA_LR_MOD), (3) a *P/S* earthquake and explosion velocity-tomography model (DVESA_LOTOS_MOD), (4) a first-order *P*-velocity model estimated from *P*-autocorrelation beam forward modeling (DVSA_ACOR_MOD), and (5) a *P/S*-velocity model inverted from phase velocity measurements at ad-hoc arrays in the study area (DVSA_PHVEL_MOD). All the estimated *P/S* velocity models are currently integrated using a set of algorithms named MAT_MOD, which is described below. The resulting model will be the input model in the inversion to complete the final high resolution DVSA *P/S* seismic model.

Tomographic models have edge effects, due to limited information availability close to the model boundary. This is why we consider an extended study area with a network of 120 broadband and short-period stations (DVESA) including 42 three-component broadband station locations that comprise the 2011-2012 ambient seismic noise survey deployment (Figures 1 and 2). For the entire study, GFs are extracted on more than 1200 inter-station paths, including the ray paths shown in Figure 2. Data is processed using ambient seismic noise and signal autocorrelation and crosscorrelation algorithms in a package of optimized analysis codes (Tibuleac *et al.*, 2011; Tibuleac and von Seggern, 2012).

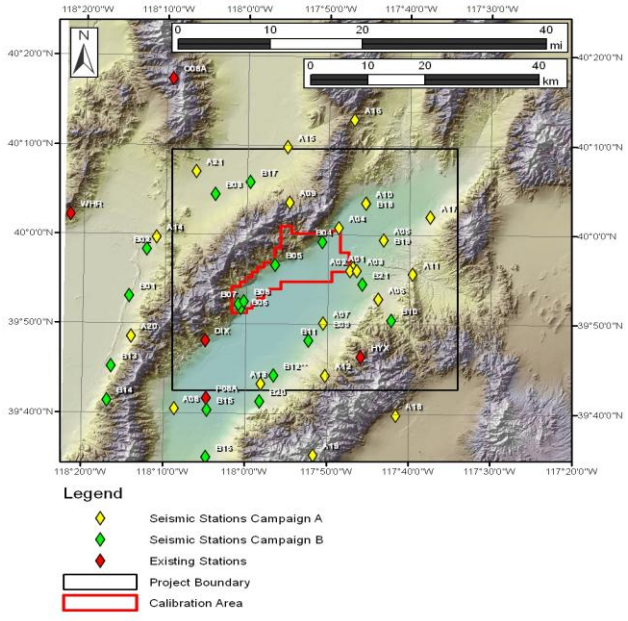

Figure 1: Map of the seismic survey locations in the Dixie Valley Study Area (DVSA) also referred to as the EGS Exploration Methodology Project Area (black outline). The Dixie Valley Geothermal Well field (DVGW) named "the calibration area" is shown in red.

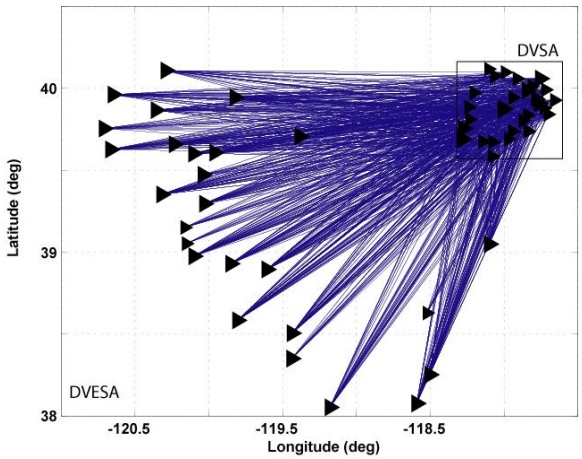

Figure 2: Ambient seismic survey station locations (triangles) in the Dixie Valley Study Area (DVSA), the Nevada Network permanent station locations in which operated during the DVSA seismic deployment in the extended Dixie Valley Study Area (DVESA), and some of the inter-station ray paths used in this study. GF's extracted on the paths shown here are used to estimate DVESA_LR_MODEL as well as DVSA_PHVEL_MODEL.

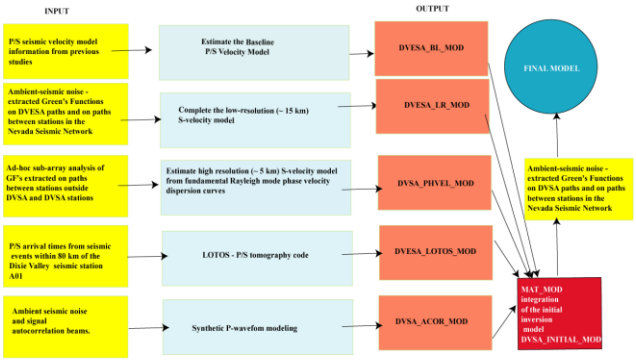

Figure 3. The analytical method used to generate a final seismic model.

The autocorrelations are estimated at all stations for a sample rate of 100 sps, in an effort to obtain better resolution of the layers below each station. A sample rate of 20 sps is considered high enough for crosscorrelations, for station spacing which ranges from 1 to 75 km in the DVSA, since the observed Rayleigh waves have periods lower than 0.2 seconds.

RESULTS

High resolution seismic velocity model estimation in the DVSA

The GFs extracted between pairs of stations in DVSA are shown in Figure 4. An approximate 5km resolution *P/S* velocity model is estimated using 396 highest signal-to-noise ratio (SNR) inter-station GFs extracted in the study area (DVSA). Fundamental Ray-

leigh group velocity dispersion curves are estimated and inverted using the CPS3.3 algorithms *do_mft* and *surf96* (Herrmann and Ammon, 2002). To estimate a group velocity tomographic model and to perform grid-dispersion inversion we use the code *gridsp*, written by Dr. Hafidh Ghalib. The propagations paths are assumed to be straight rays. A stochastic inversion code is used, following a method by Feng and Teng (1983). The fundamental mode Rayleigh group velocity tomography results are shown in Figure 5. A "rule" of thumb" is that the numeric value of the period of the fundamental mode Rayleigh corresponds to the depth best sampled by a waveform (at 1/2 of the wavelength from the surface), assuming the group velocity ~ 3 km/s. Dispersion curves are analyzed at periods from 2s to 10s. The surface of the DVSA is partitioned into a grid with elements 0.05˚ on one side. A dispersion curve is estimated for each of the 140 total grid elements in the DVSA. To invert for the DVSA model, a starting P/S velocity model named DVSA_INITIAL_MODEL (Figure 3, lower right) is needed. This model is extracted from the compilation of all available current velocity models in the area, as described below. We are currently completing estimation of the final *P/S* velocity maps to be used as input into the final DVSA *P/S* seismic velocity model inversion.

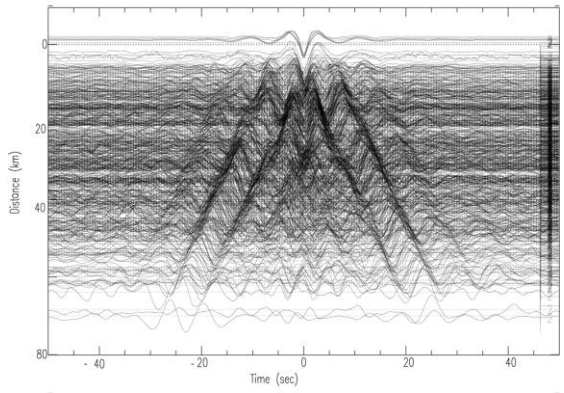

Figure 4. Record section of raw, two-sided GFs extracted in the DVSA area. The vertical axis shows inter-station distance. Fundamental mode Rayleigh traveling with a group velocity of ~ 3 km/s are the largest arrivals at all distances. The DVSA ambient seismic noise field and the seismic signals are approximately isotropic, as shown by symmetrical waveforms on one side and the other of the zero time lag.

Estimation of the DVSA_INPUT_MODEL

Generating a higher resolution DVSA input model (DVSA_INPUT_MODEL) is the focus of our efforts, as a necessary step before estimation of the final DVSA model. Such a detailed seismic shear velocity model was not available in the area. High resolution (hundreds of meters) *P*-velocity models were available only from reflection lines, as concluded after the EGS Baseline Geothermal Conceptual Model (in prep) *P/S* velocity model estimation (DVESA_BL_MOD in Figure 3). New, higher resolution, independent *P/S* velocity model estimates are integrated into the DVSA_INPUT_MODEL, using a new set of Matlab algorithms named MAT_MOD.

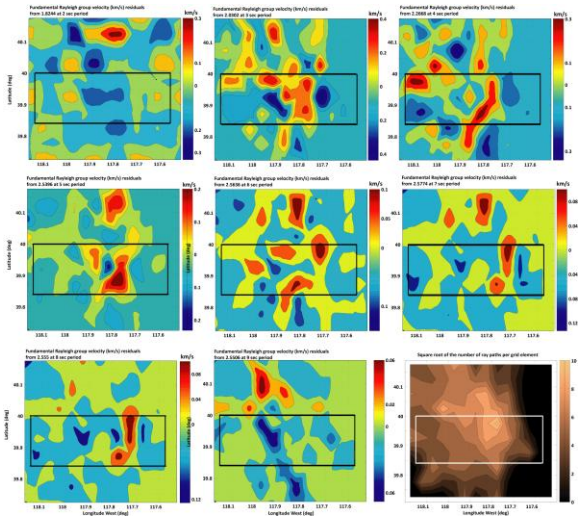

Figure 5. All plan-view plots, except for the lower right plot, show fundamental mode Rayleigh group velocity maps in DVSA at periods of 2-10s. For waveforms with group velocity ~ 3 km/s the rule of thumb is that the best sampled depth has a numerical value similar to the period. The DVSA area is shown as a black rectangle in each plot. The lower right plot shows log10 of the inter-station path density in the area. The best resolved regions (light color) are intersected by the largest number of ray paths.

MAT_MOD

Each model we collect or estimate is stored into a Matlab "structure". A "structure" is a named collection of data representing a single idea or "object". The structure contains a list of fields, each being a variable name for some sub-piece of data. Structures are similar to arrays in that they contain multiple data, but the main difference is, instead of an index to each piece of data, we have a "name"; and instead of every piece of data being the same type, we can have a different type for each "field". The fields of a MAT_MOD structure are: the reference to the model; the model area (which is a square oriented North-South, East-West; and the model matrix. The model matrix has eleven columns: depth, *P*-velocity in km/s, *S*-velocity in km/s, density (g/cm^3), *P* and *S* attenuation factors *Qp* and *Qs* and five trust factors, one for each *P*, *S*, density, *Qp* and *Qs*. For "no information" the matrix element value is set to -99. The "trust" factor ranges from 0 to 1 and is, for example, set by the analyst up to 0.9 for reflection/refraction lines and is set to 0.01 for general (non-local) models. Using the "trust" parameter, seismic lines and local data are given higher weights than the global model weights.

A "slack" number (in this case 0.05˚) for each model represents the area where the model is considered valid. When, for example, the P/S-velocity model at a point characterized by a location (latitude, longitude) is requested by the user, MAT_MOD finds all the models including a square centered on the respective point, i.e within 0.05˚ from the respective point. A side of the square is twice the slack number value. For example, the resulting *P*-velocity at the respective point is a "trust" - parameter weighted mean, after the "-99" estimates are discarded. The MAT_MOD algorithms were particularly suitable for this study, because they allowed integration of independent information from multiple sources.

DVESA_BL_MOD

An initial, low-resolution (~ 40 km) *P/S* seismic velocity model of the area (DVESA_BL_MOD, see Figure 3), presented in the EGS Baseline Geothermal Conceptual Model is estimated using all the existing literature and all the experimental information. Publicly available velocity models are used to build this model, with crust-mantle boundary (Moho) discontinuity constraints and with seismic attenuation information. Two improved resolution (~ 30km), University of Nevada Reno (UNR)-estimated, velocity models in Nevada were added to the DVESA_BL_MOD (1) a low resolution (30-50km), Nevada *P/S* seismic velocity model by Preston and von Seggern (2003) and (2) a *P/S* model estimated by Biasi *et al.* (2010).

Table 1. Mean shear velocity models extracted from the dispersion curves in DVESA and DVSA (see text for an explanation), the model used to generate a synthetic reflection waveform shown in Figure 13 and the starting model for DVESA shear velocity inversion.

	DVESA	DVSA	Synthetic waveform empirical model: DVSA_ACOR_MOD		Initial model for DVESA_LR_MOD *P/S* seismic velocity model inversion
Layer thickness (km)	S-vel (km/s)	S-vel (km/s)	P-vel (km/s)	S- vel (km/s)	S-velocity (km/s)
1	1.4	1.4	2.1	1.0	2.2
1	1.5	1.6	3	2	2.2
2	2.0	1.9	5.2	3.1	2.5
2	2.5	2.5	5.6	3.4	2.9
2	3.3	3.5	5.6	3.4	3.6
12			5.5	3.3	
8			7.4	4.0	

DVESA_LR_MOD

A new, improved resolution (~ 0.15˚) seismic velocity model in the DVESA (DVESA_LR_MOD) is extracted from 1285 interstation GF dispersion curves estimated from ambient seismic noise and signal, on paths including those shown in Figure 2. Vertical component GFs used to estimate this model are shown in Figure 6, with fundamental mode Rayleigh waves as the largest arrivals. More than 1280 dispersion curves are used.

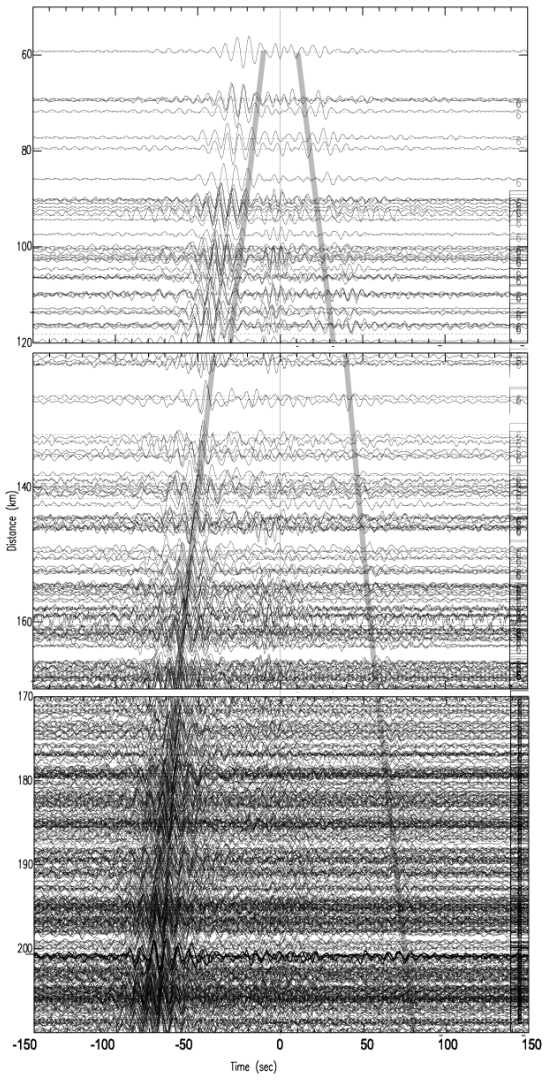

Figure 6. Record section of two-sided, raw, vertical component GFs extracted in the DVESA area (Figures 1 and 2). The vertical axis shows the interstation distance. Fundamental mode Rayleigh traveling with a group velocity of ~ 3 km/s are the largest arrivals at all distances. The gray lines show the 3 km/s arrival time. If the seismic "noise" would be isotropic, each GF would be symmetrical with respect to the zero lag. Noise directionality, i.e., more energy propagating from the Sierra Nevada to DVSA compared to the energy propagating in the opposite direction, results in asymmetrical GFs.

With the same method as for DVSA, fundamental mode Rayleigh wave group velocity maps are estimated at periods from 4s to 20s and selected periods are illustrated in Figure 7. The DVESA surface is partitioned into a grid with elements 0.15˚ on one side. A dispersion curve is interpolated and inverted for a seismic velocity model for each of the 572 grid elements. Shear-wave velocity models estimated at 5km, 7km, 10km, 15km and 20km depth from the surface are shown in Figure 8. The initial model for DVESA_LR_MOD is similar to models in Priestley and Brune (1978) and Tibuleac et al. (2012) (Table 1).

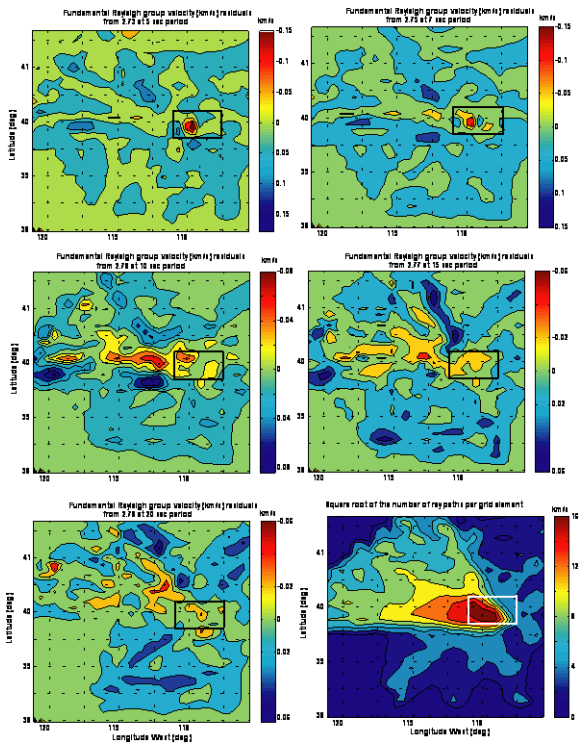

Figure 7. Fundamental Rayleigh group velocity maps at periods of 5s, 7s, 10s, 15s and 20s in the DVESA. The DVSA area is shown as a black rectangle in each plot. The lower right plot shows the square root of the number of paths per grid element used to estimate the velocity models, and DVSA in a white rectangle. Note that the paths shown in the lower right plot include the paths shown in Figure 2, and inter-station paths for pairs of stations from past deployments in the region, such as the USArray deployment (between years 2006 and 2009).

DVESA_LOTOS_MOD

Precise location of the events used for tomographic inversion is one of the most important conditions for accurate velocity model estimates. Local events, earthquakes and explosions, which occurred during the 2011-2012 ambient seismic noise (passive) survey deployment in DVSA (Figure 1), have been detected and located, up to 80 km from DVSA station A05, in an area from 39.25N to 40.65N and from 117.15W to 118.55W. As expected, the incorporation of the DVSA array data provides a significant improvement over the Nevada Seismological Laboratory (NSL) locations. Because of poor permanent Nevada Network station coverage in the DVESA, larger DVESA earthquake epicenters are mislocated by NSL by up to 20 km. Explosions are not analyzed at NSL. DVESA mining and military explosions are identified and their locations are corrected. We also locate small magnitude earthquakes which occurred in DVSA. A total of 43 events have well-defined *P*- and *S*- arrivals.

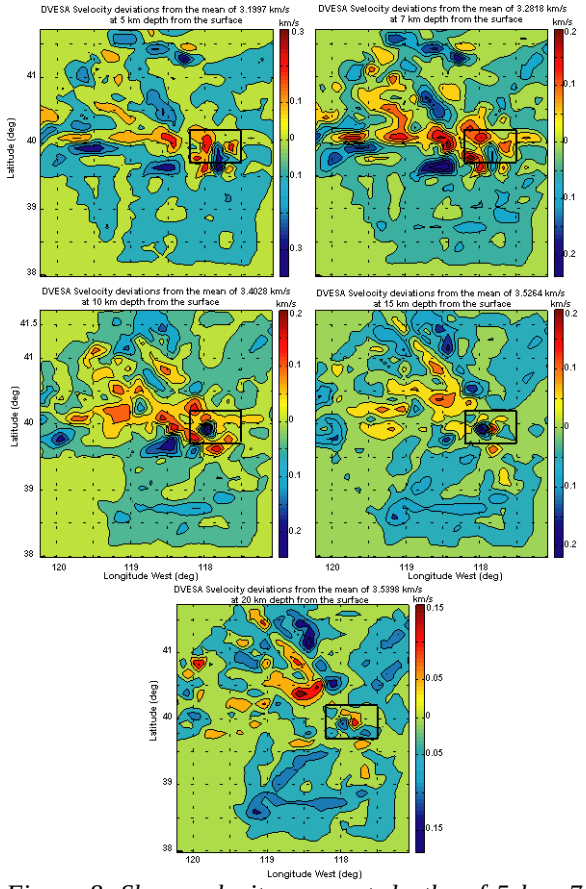

Figure 8. Shear velocity maps at depths of 5 km, 7 km, 10 km, 15 km and 20 km. The DVSA area is shown as a black rectangle in each plot. Results provide important DVSA_INITIAL_MODEL constraints and can be used for comparison of the seismic experiment results with results of other geophysical studies.

A set of tomographic inversion algorithms, *LOTOS-10* for 3D tomographic inversion (Koulakov, 2009) is used. One of the key features of the *LOTOS-10* code is a ray tracing algorithm based on the Fermat principle of travel time minimization called bending tracing (see Koulakov, 2009). Elevation corrections are applied using an empirically chosen replacement velocity of 4 km/s relative to the station A05 elevation.

Thus, the depth of the estimated *P/S* velocity model (DVESA_LOTOS_MOD) is from surface.

The inversion for *P/S* velocity anomalies is performed by LOTOS in several steps: 1) Simultaneous optimization for the best 1D velocity model and preliminary relocation of sources; 2) Re-location of sources in the 3D velocity model; and 3) Simultaneous inversion for the source parameters and velocity model using several parameterization grids. Steps 2 and 3 are repeated in five iterations. The input (gray) and final (red) mean *P/S* wave seismic velocity model (estimated at step 1) in the LOTOS study area are shown in Figure 9.

Examples of vertical sections and of horizontal model cross-sections at 3 km depth are shown in Figures 10 and 11. The velocity anomalies in each horizontal and vertical section are estimated as percentages of the reference model velocity at the respective depth. More than 600 *P*- and over 100 *S*-arrival travel time measurements are used as input to LOTOS. The DVESA_LOTOS_MOD is the *P/S* seismic velocity model estimated from LOTOS-inversion. Figure 11 shows vertical sections through the model and a map with the location of the sections. We observe that the *P/S* velocity anomalies change sign at the location of the DVSA earthquakes. A disadvantage of using LOTOS in the DVSA is that the best model resolution (with most uniform grid coverage) is obtained at 5-8 km (which is actually the depth range of the DVSA earthquakes). At 1-4 km depth, the grid nodes used in calculations are concentrated within 3 km of each station, thus, despite the fact the *P/S* velocity models are smoothed to show continuous velocity variation, the model best describes subsurface features in the vicinity of the station.

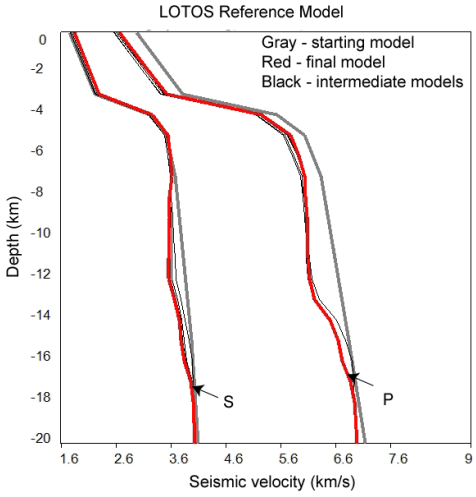

Figure 9. The mean P/S wave seismic velocity model in the DVESA area, estimated with LOTOS (see text for explanation). Gray shows the starting model, the intermediate models are shown as thin lines and red is the final model. Note low P-velocity in the mid-crust at ~12 km, which is confirmed by autocorrelation and phase velocity results, as shown below.

DVSA_ACOR_MOD

Autocorrelation beam analysis at each DVSA station is conducted to develop the DVSA_ACOR_MOD (Figure 3). However, prior to analysis of nearly-vertically propagating waveforms, such as those extracted from autocorrelation beams, corrections must be made for elevation and complex geology beneath each station to the *P*-travel times recorded at an array (Tibuleac et al., 2001).

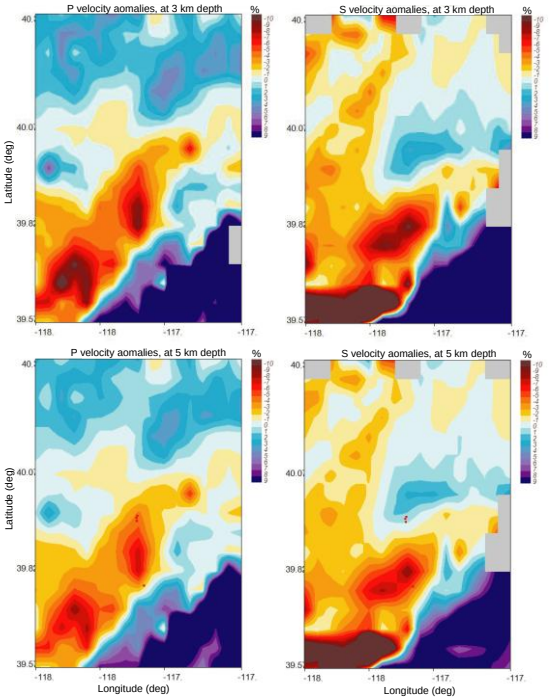

Figure 10. Upper plots: Example of LOTOS results at 3 km depth. The left plot shows the estimated P-wave velocity anomalies (%) and the right plot shows the estimated S-velocity anomalies (%) when compared to the reference model at 3 km depth (Figure 9). Lower plots: Same as in the upper plots at 5km depth. Large S-velocity anomalies at the bottom of each figure are probably edge effects.

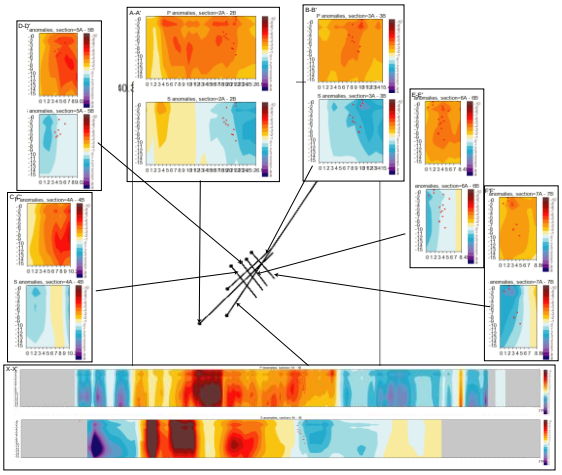

Figure 11. Vertical cross-sections (to a depth of 20 km) in the Dixie Valley calibration area for sections shown in the middle plot. In each inset, the upper plot shows P - velocity model anomalies (%) relative to the reference model in Figure 9 and the lower plot shows the estimated S-velocity model anomalies (%) relative to the same model, at each depth. The red dots are earthquakes re-located within 2 km of the vertical section. Note that only sections crossing the within 2 km of the hypocenter show the earthquake location.

Static corrections for P-arrivals

The elevation difference between the DVSA ambient seismic noise survey stations is generally less than 200 m, however, three stations are up to 1200m higher elevation than the majority of stations. Also, the geologic structure varies beneath each station. Simple *P*-phase travel time corrections using a replacement velocity (Lindquist et al, 2005) do not remove geology and elevation caused time delays. Thus, static corrections to *P*-wave arrivals are estimated at all stations (Figure 12).

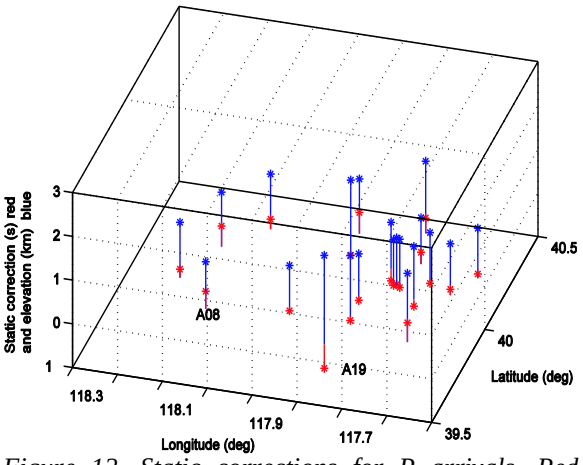

Figure 12. Static corrections for P arrivals. Red segments show the static corrections (s) at each station, blue segments show the elevation (km).

Teleseismic earthquake waveform crosscorrelations, with reference station A05 (Figure 1), which is the lowest elevation station, are used to estimate static corrections. The teleseism locations are chosen such that the waveforms are arriving nearly vertically at the stations. After applying corrections for horizontal propagation using the United States Geological Survey estimated slowness (the inverse of the *P*-horizontal velocity), static corrections are estimated at every station as a mean for over 100 teleseisms. The static correction value varies from -0.55s at A09, to 0.48s at A15. Static corrections do not show a pattern either as a function of elevation, known geology, or known temperature distribution.

Autocorrelations

Autocorrelation beams, representing the P-reflection GF component beneath each station are processed for supplementary constraints on subsurface features. A synthetic waveform is estimated for an empirical velocity model (Table 1). The model provides a good approximation of the geologic formations beneath each station, once the static corrections (Figure 12) are applied. A possible explanation is that, except for variations within the first 1-2 km, the reflectors in the DVSA may be at similar depth intervals. This affirmation, however, needs to be supported by supplementary synthetic modeling evidence, which is the object of further investigations. Figure 13 shows a comparison of a synthetic waveform and the autocorrelation beams along a line of stations to the east of the Stillwater Range, crossing the DVSA calibration area.

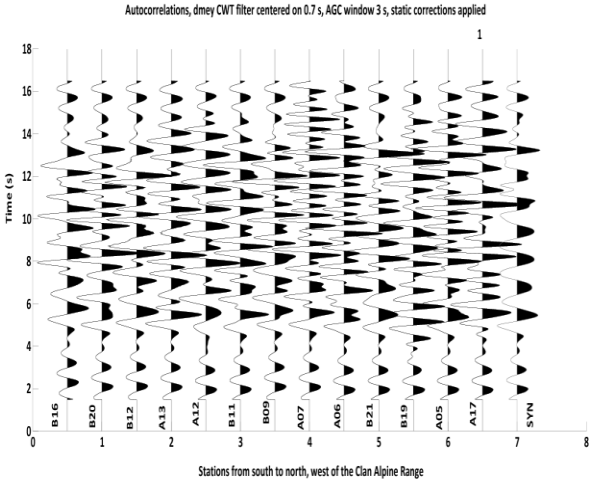

Figure 13. An example of autocorrelation beams extracted on a profile west of the Clan Alpine Range, including stations B16, B20, B12, A13, A12, B11, B9, A7, A6, B21, B19, A5 and A17 (see Figure 1 for station locations). Automatic gain control (AGC) was applied in a window of 3s on each trace. The waveform to the right is synthetic. Note a clear arrival at ~6s, possibly a reflection from a layer ~10 km deep. We observe that the lower the frequency band of the filter applied to the waveforms before AGC, the deeper are the layers we interpret as being resolved by the GF P-reflection components.

DVSA_PHVEL_MOD

Lines and ad-hoc sub-arrays of stations are identified for GF investigation using array processing techniques (Tibuleac et al., 2011). A GF is extracted for each path between (1) a DVSA station in a sub-array. The sub-arrays are selected based on conductive heat flow modeling (Blackwell, 2007; Thakur *et al.*, 2012), or to include wells of interest in the focus area; and (2) one of the available 22 permanent seismic stations in the DVESA. The selected far DVESA station is considered the virtual source of an "event"

recorded at the ad-hoc DVSA sub-array. A fundamental mode Rayleigh phase velocity dispersion curve is extracted, which depends on the subsurface structure at the sub-array. GFs were analyzed from paths including a total of 22 far-stations in and in the vicinity of DVESA, at 30 ad-hoc-arrays in the DVSA. Figure 14 shows examples of frequency-wavenumber (*fk*) analysis for virtual sources at stations WVA and SBT and virtual receivers in the DVSA. Fundamental mode Rayleigh phase velocity dispersion curves in DVSA (see Figure 15 for examples) are currently being inverted for shear-wave velocity models. These models are integrated into the DVSA_PHVEL_MOD (Figure 3).

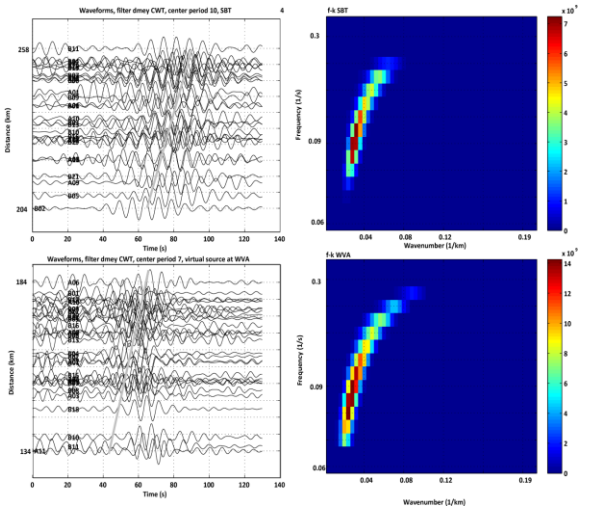

Figure 14. Example of frequency-wavenumber (fk) analysis for stations virtual sources at stations WVA and SBT and virtual receivers in the DVSA. The gray line shows the 3km/s time marks in the left plots. Left plots show the GF waveforms, scaled to the maximum value. The right plots show the fundamental mode Rayleigh-wave phase velocity estimated at the entire DVSA array. Waveforms are filtered using a Continuous Wavelet Transform with a Meyer wavelet centered on 10 (upper right plot) or 7s (lower left plot) period as indicated on the plot. The "hot" (towards red) colors on the fk plots show the maximum-energy value for each wave number and frequency value.

FUTURE WORK

We have presently assembled the DVSA_INPUT_MODEL. Final investigations include using this model as the initial model in the inversion for the final DVSA velocity model (Figure 3, right). The model will be integrated into a Matlab environment and will be provided to AltaRock for integration with the results of the other geophysical methods.

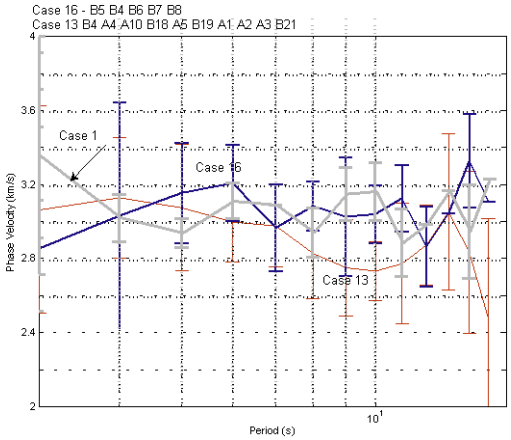

Figure 15. Fundamental mode Rayleigh phase velocity dispersion curves (named FMRPHD) extracted using frequency-wavenumber (fk) analysis from ad-hoc sub-arrays of stations in DVSA (see Figure 1 for station locations). Each line follows the mean of all the measured phase velocity values for an ad-hoc array, represented for each period, and the standard deviation at each period is shown as vertical bars. Gray shows the FMRPHD when the sub-array includes all the DVSA stations. This is a mean FMRPHD for the Dixie Valley. Blue shows FMRPHD for a line of stations on the eastern flank of the Stillwater range, southwest of the Stillwater power plant location (including well 45-14). Red shows the FMRPHD beneath a small sub-array NE of the Stillwater geothermal power plant, including well 66-21. For this NE sub-array, note lower velocities in the 8-12s period range, which are usually inverted into low S-velocity models in the upper crust at depths of approximately the same numerical value as the periods. These dispersion curves are currently inverted to obtain shear velocity variation with depth and estimate DVSA_PHVEL_MOD.

REFERENCES

Biasi, G., Preston, L., and Tibuleac, I. M, 2009, Body Wave Tomography for Regional Scale Assessment of Geothermal Indicators in the Western Great Basin, Geothermal Resources Council Transactions, v. 33, p. 437-440.

Blackwell, D. D., R. P. Smith, and M. C. Richards, Exploration and development at Dixie Valley, Nevada: summary of DOE studies: Proc. 32nd Workshop on geothermal reservoir engineering, Stanford Univ., CA, SGR-TR-183, 16 pp., 2007.

Catchings, R. D., and W. D. Mooney, Basin and Range crustal and upper mantle structure, northwest to central Nevada: J. Geophys. Res., 96, 6247-6267, 1991.

Feng, C. C. an T. L. Teng (1983). Three-dimensional crust and upper mantle structure of the Eura-

sian continent, J. Geophys. Res., 88, 2261-2272.

Herrmann, R. B., and C. J. Ammon (2002). Computer Programs in Seismology – 3.30: Source inversion, available at URL: http://www.eas.slu.edu/People/RBHerrmann/CPS330.html, 99.

Iovenitti, J.L., Blackwell, D.D., Sainsbury, J.S., Tibuleac, I.M., Waibel, A.F., Cladouhos, T.T., Karlin, R., Kennedy, B.M., Isaaks, E., Wannamaker P.E., Clyne, M.T., Ibser, F.H., Callahan, O.C., 2012, Towards Developing a Calibrated EGS Exploration Methodology Using the Dixie Valley Geothermal System, Nevada. Proceedings, Thirty-Seventh Workshop on Geothermal Reservoir Engineering Stanford University, Stanford, California, January 30 - February 1. 15 p.

Koulakov I., 2009, LOTOS code for local earthquake tomographic inversion. Benchmarks for testing tomographic algorithms, Bulletin of the Seismological Society of America, Vol. 99, No. 1, pp. 194-214, doi: 10.1785/0120080013

Lindquist, K. G., Tibuleac, I. M. and R. A. Hansen (2005). A Semi-Automatic Calibration Method Applied to a Small-aperture Alaskan Seismic Array, Bull. Seism. Soc. Am. 97, pp. 100.

Priestley, K and J. Brune, 1978. Surface waves and the structure of the Great Basin of Nevada and western Utah, JGR, v. 83, pp. 2265-2272.

Preston, L., and D. von Seggern, Joint Seismic Tomography/Location Inversion in the Reno/Carson City Area, Final Report to the National Earthquake Hazard Reduction Program, U. S. Geological Survey Award Number 07HQGR0022, 2008.

Thakur, M., Blackwell, D. D., and Erkan, K. (2012) "The Regional Thermal Regime in Dixie Valley, Nevada, USA," *Geothermal Resources Council Transactions*, v. 36, p. 59 – 67.

Tibuleac and von Seggern, in prep, An inexpensive, non-invasive method to estimate P/S seismic velocity models in the highly populated Reno Basin area, using ambient - seismic noise and signalin preparation for Seismological Research Letters

Tibuleac, I. M, E.T. Herrin and P. Negraru, (2001). Calibration Studies at NVAR, Seis. Res. Lett. 72, 754.

Tibuleac, I. M. and D. H. von Seggern, Crust-mantle boundary reflectors in Nevada from noise auto-correlations, 2012, Geophys. J. Int., Vol. 189, Issue 1, pp. 493-500.

Tibuleac, I. M., D. H. von Seggern, John G. Anderson and J.N. Louie, 2011. Computing Green's Functions from Ambient Noise Recorded by Narrow-Band Seismometers, Accelerometers, and Analog Seismometers, doi: 10.1785/gssrl.82.5.661 Seismological Research Letters September/October 2011 v. 82 no. 5 p. 661-675.

ACKNOWLEDGEMENTS

This work has been conducted under the American Recovery and Reinvestment Act (ARRA) funding through the U.S. Department of Energy (DOE) and AltaRock Energy Inc., DOE contract no. DE-EE0002778. We are grateful for help and advice from Dr Hafidh Ghalib. We thank the crew from Geotech Instruments, LLC and the Altarock personnel who installed and serviced the seismic stations in Dixie Valley, working in harsh high desert conditions. We thank Drs Lani Oncescu and Mihaela Rizescu from Geotech Instruments, LLC for assistance with data processing programs. We thank Gabe Plank from UNR, who helped solve computer-related problems.